ACS Sustainable Chemistry & Engineering

Research Article

Cite This: ACS Sustainable Chem. Eng. 2018, 6, 13096−13106

pubs.acs.org/journal/ascecg

Making Benzoxazines Greener: Design, Synthesis, and Polymerization of a Biobased Benzoxazine Fulfilling Two Principles of Green Chemistry

María Laura Salum,[†,§] Daniela Iguchi,[†,‡] Carlos Rodriguez Arza,[†] Lu Han,[†] Hatsuo Ishida,*[,†] and Pablo Froimowicz*[,†,‡]

[†]Department of Macromolecular Science and Engineering, Case Western Reserve University, 2100 Adelbert Road, Cleveland, Ohio 44106-7202, United States

[‡]Design and Chemistry of Macromolecules Group, Institute of Technology in Polymers and Nanotechnology (ITPN), UBA-CONICET, FIUBA, FADU, University of Buenos Aires, Intendente Güiraldes s/n, Pabellón III, Subsuelo, Ciudad Universitaria (1428), Buenos Aires, Argentina

ABSTRACT: Sesamol and furfurylamine are used to synthesize a novel benzoxazine monomer as part of the quest to develop greener benzoxazine monomers simultaneously fulfilling two Principles of Green Chemistry, the *use of renewable feedstocks* and *safer solvents and auxiliaries*. Respecting principle 5, the so-called *preferred* solvents (ethanol and ethyl acetate) are used in both the syntheses and purification processes. The chemical structure of the synthesized monomer is verified by proton and carbon nuclear magnetic resonance spectroscopy (^{1}H and ^{13}C NMR), 2D ^{1}H−^{13}C heteronuclear single quantum correlation (HSQC) spectroscopy, and Fourier transform infrared spectroscopy (FT-IR). The polymerization behavior of the monomer and the thermal stability of fully polymerized polybenzoxazine are studied by differential scanning calorimetry (DSC) and thermogravimetric analysis (TGA). A thermally stable polymer has been obtained as shown by the 5% and 10% weight reduction temperature (T_{d5} and T_{d10}) values of 374 and 419 °C, respectively, and a char yield of 64%, making this thermoset a promising candidate for fire-resistant applications.

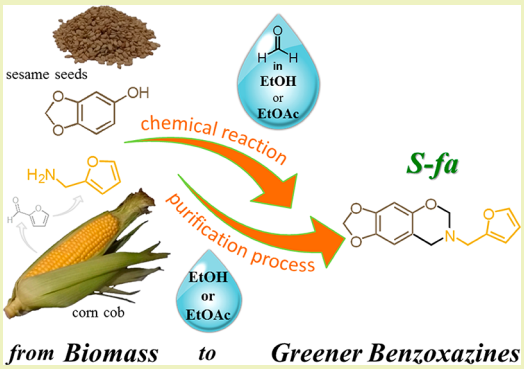

KEYWORDS: *Natural renewable resources, Green solvents, Chemical design, Benzoxazine chemistry*

INTRODUCTION

Small molecular weight benzoxazines have been known for a long time, covering various fields of study,[1] such as reducing agents,[2] optoelectronic materials,[3] antimicrobial systems,[4] medicine,[5] and monomers for the production of polymers. This last area, although the history is much shorter than other areas, is of particular interest because its broadness has enabled the development of an entire new research field, with demonstrated great interest from both the industrial and the scientific arenas. Thus, the so-called benzoxazine and polybenzoxazine fields have established themselves as independent research fields within the polymer arena since 1994,[6] finding a variety of subdisciplines. Some examples are the synthesis and study of symmetrical versus asymmetric resins,[7] monomers introducing specific functionalities or reactivity by design,[8−10] higher thermal stability,[11−14] and, more recently, smart materials including stimuli-responsive systems,[15,16] fire smart materials,[17] self-healing materials,[18] and shape-memory materials.[19] Replaceability of petroleum-based starting materials by those coming from natural and renewable resources for the synthesis of new monomers is drawing particularly strong interest from both industry and academia.[20,21]

This last example, although very important, has somehow introduced a conceptual misinterpretation in the literature, where the simple fact of using natural renewable raw material is wrongly taken as a synonym of carrying out Green Chemistry. The use of these biobased raw materials is, according to the renowned authors of the book, Anastas and Warner, just one of the Principles of Green Chemistry, principle number 7.[22] A similar situation has been observed in the case of performing a solventless chemical reaction. What needs to be stressed in this point is that a chemical reaction, even a one-pot reaction, involves different components and stages. In other words, a chemical reaction essentially includes the following: (1) the reactant or reactants for the chemical reaction itself and the product(s) (and possibly catalysts or initiators); (2) the solvent in which such a reaction is carried out (although not always present); and (3) solvent(s), other chemicals, auxiliaries (resins and silica gel, for instance), or even methods used for the purification step or steps (recrystallizations and chromatographies, for example) normally performed using solvents,

Received: June 5, 2018
Revised: August 13, 2018
Published: August 15, 2018

DOI: 10.1021/acssuschemeng.8b02641
ACS Sustainable Chem. Eng. 2018, 6, 13096−13106

Table 1. Phenol and Amine Reactants, Reaction Solvents, and Purification Solvents Used for the Synthesis of Related Biobased Benzoxazines

no.	phenol	amine	reaction solvent	purification solvent	ref
1	terpene diphenol	aniline	1,4-dioxane	no purification was carried out	28
2	coumarin	*p*-toluidine	1,4-dioxane + MeOH	washed from $CHCl_3$ recrystallization from THF	29
3	cardanol	aqueous solution of ammonia	aqueous solution of ammonia	washed from $CHCl_3$ column chromatographed with $CHCl_3$	30
4	cardanol	various	no solvent	when purified, column chromatographed with $CHCl_3$	31
5	cardanol	aniline	no solvent	extracted with $CHCl_3$	32
6	cardanol	aniline	no solvent	extracted from ether (no further specification)	33
7	diphenolic acid	aniline	toluene	extracted from ethyl ether	34
8	*p*-cresol	glycine	ethanol	no purification was carried out	35
9	cardanol	diaminodiphenylmethane	no solvent	extracted from ethyl acetate	36
10	urushiol	aniline	1,4-dioxane	extracted from dichloromethane then chromatographed, but no solvent was specified	37
11	guaiacol	furfurylamine stearyl amine	no solvent no solvent	no work up carried out crystallized from ethanol crystallized from ethanol	25
12	guaiacol	furfuryl amine	ethanol	recrystallized from ethanol	26
13	ferulic acid	1,3,5-triphenylhexahydro-1,3,5-triazine	toluene	washed from diethyl ether recrystallized using heptanes/1,2-dichloroethane 7:3 mixture	38
14	eugenol	bis(4-aminophenyl)ether	dimethylsulfoxide	precipitation in water with no further purification	39
15	eugenol	stearyl amine	no solvent	crystallized from ethanol	40
16	rosin	aniline	dimethylformamide	extracted from dichloromethane	41
17	eugenol	1,4-phenylenediamine	no solvent	extracted from $CHCl_3$ no further purification	42
18	cardanol	furfuryl amine	no solvent	no purification was carried out	43
19	arbutin	furfuryl amine	no solvent	crystallized from ethanol	27
20	chavicol	1,4-phenylenediamine	no solvent	crystallized from ethanol	44
21	bakuchiol	25 different amines	THF/MeOH	column chromatographed using EtOAc/hexane (1:49)	5

which can be the same as the ones used in the reaction but not necessarily.

A survey of biobased benzoxazine syntheses is summarized in Table 1 showing natural renewable raw materials (phenol, amine, or both), the solvent used in the reaction system, and the solvent/solvents utilized in the purification processes. It can be seen in the table that most of those syntheses were carried out in solvents actually classified as undesirable[23,24] when following recommendations from the Principles of Green Chemistry,[22] while a few others were in accepted ones although the purifications were done once again using undesirable solvents. In the case of the few examples of solventless reactions, the purifications were performed using those undesirable solvents. In consequence, the synthesis of resins as a whole, in other words the actual synthesis pathway followed, should not be classified as Green Chemistry. The use of little volumes of acceptable solvents or the utilization of solventless systems for carrying out a given chemical reaction to then be forced to use large volumes of unhealthy and contaminant solvents should be discouraged. The only exceptions observed within the examples are those shown in entries 11[25] and 12,[26] which are reported by the same group, and 19.[27] However, the important role played by the solvents (reaction and purification) in those syntheses was practically overlooked. It is precisely in this context that the present work is aimed at establishing the bases for obtaining novel high-end materials following greener synthetic procedures. Therefore, this research proposes not only to use precursors coming from the biomass (Principle of Green Chemistry number 7) but also to go one step further and react them and then purify the product(s) using only those solvents classified as preferred[23,24] (principle of Green Chemistry number 5[22]). Clearly, the objective of the present work is not to right away fulfill simultaneously all 12 Principles of Green Chemistry but rather to incorporate the second one to the one that has been carried out hitherto in the literature.

As a high-end material, we targeted the synthesis of a thermally stable thermoset polymer to evaluate it as a potential candidate toward flame-retardant material. Sesamol and furfurylamine were used as raw materials for the synthesis of the resin, being both compounds that are easily obtainable from natural renewable resources.[45,46] The extraordinarily rich molecular-design flexibility of benzoxazine resins allowed us to plan a realistic synthetic pathway taking into consideration all objectives proposed simultaneously. Thus, the production of a biobased benzoxazine using only the most preferred solvents[23,24] as recommended by the Principles of Green Chemistry[22] both in its synthesis and in the purifications is performed. It is important to note that neither the reaction yield nor the level of purity obtained for the herein presented resin were sacrificed by the incorporation of this greener methodology. Finally, the thermal stability studies of the resulting polymer were carried out where a high thermal stability and an unexpected very high char yield were observed. These results are comparable to, or even higher than, those of other polybenzoxazines obtained with precursors of the traditional petrochemical and other biobased ones previously reported.[21]

DOI: 10.1021/acssuschemeng.8b02641
ACS Sustainable Chem. Eng. 2018, 6, 13096−13106

Scheme 1. Synthesis of Benzoxazine Monomer S-fa, Showing Two Possible Isomers Formation and the Mixture of Them

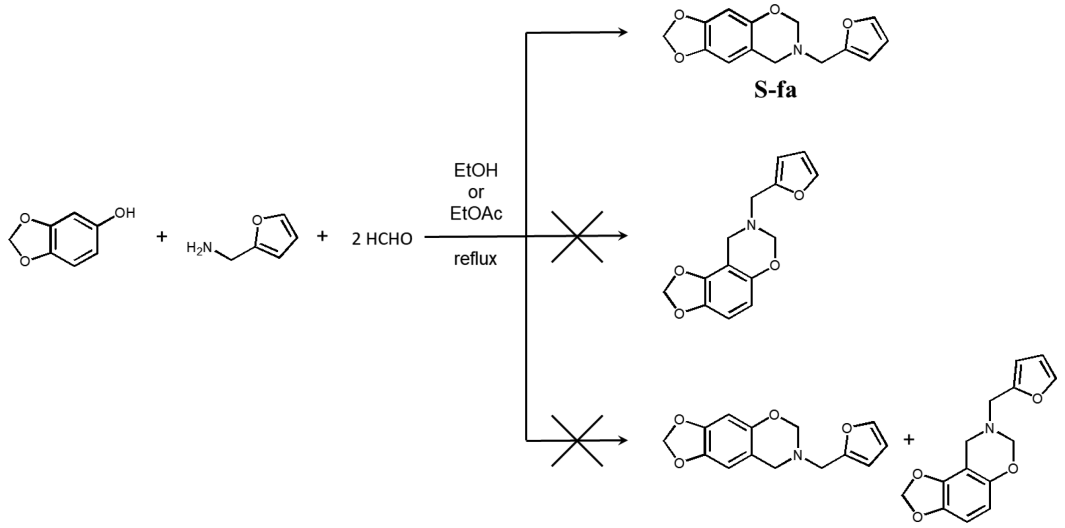

EXPERIMENTAL SECTION

Materials. Sesamol (>98%), furfurylamine (98%), and paraformaldehyde (96%) were used as received from Sigma-Aldrich. Ethanol, ethyl acetate, sodium hydroxide (NaOH), and magnesium sulfate ($MgSO_4$) were obtained from Fisher Scientific and used as received.

Synthesis of 7-(Furan-2-ylmethyl)-7,8-dihydro-6*H*-[1,3]-dioxolo[4′,5′:4,5]benzo[1,2-*e*][1,3]oxazine (hereinafter abbreviated as S-fa). *Method 1: Ethyl Acetate As a Solvent.* To a dispersion of sesamol (4.00 g, 30.00 mmol) and paraformaldehyde (1.92 g, 63.9 mmol, 2.1 equiv) in ethyl acetate (150 mL) was added furfurylamine (2.94 g, 30.27 mmol). The reaction mixture was heated in a 250 mL round-bottom flask equipped with a magnetic stirrer and was heated to reflux overnight. The reaction mixture was washed three times with 1 M NaOH aqueous solution, dried over anhydrous $MgSO_4$, and filtrated. Removal of the solvent using a rotary evaporator yielded white crystals. Recrystallization in a mixture of ethanol/ethyl acetate (93:7) allowed us to obtain white needle-like crystals. The reaction yield is 68%.

Method 2: Ethanol As a Solvent. The synthetic procedure followed is the same as the previous procedure, method 1, but using ethanol instead of ethyl acetate. Accordingly, sesamol (4.00 g, 30.00 mmol), paraformaldehyde (1.92 g, 63.9 mmol, 2.1 equiv), and furfurylamine (2.94 g, 30.27 mmol) in ethanol (150 mL) were kept under reflux overnight. White crystals were formed on standing. Recrystallization in a mixture of ethanol/ethyl acetate (93:7) generated white needle-like crystals. The reaction yield is 72%.

Characterization of 7-(Furan-2-ylmethyl)-7,8-dihydro-6*H*-[1,3]dioxolo[4′,5′:4,5]benzo[1,2-*e*][1,3]oxazine (S-fa). ^{1}H NMR (600 MHz, DMSO-d_6, 25 °C): δ = 7.61 (d, 1H, H_d), 6.59 (s, 1H, H_5), 6.42 (s, 1H, H_8), 6.41 (m, 1H, H_c), 6.31 (d, 1H, H_b), 5.90 (s, 2H, H_s), 4.74 (s, 2H, H_2), 3.83−3.79 (bb, 4H, H_4, and H_a). ^{13}C NMR (600 MHz, DMSO-d_6, 25 °C): δ = 151.82 (C_e), 148.01 (C_9), 146.13 (C_7), 142.61 (C_6), 141.00 (C_d), 111.08 (C_{10}), 110.38 (C_c), 108.60 (C_5), 106.76 (C_b), 100.50 (C_s), 97.98 (C_8), 81.38 (C_2), 48.68 (C_4), 47.38(C_a).

FT-IR (KBr): ν (cm^{-1}) = 1498 (furan C=C stretching), 1477 (CH_2 bending of methylenedioxybenzene group), 1442 (CH_2 bending), 1398 (C−N−C antisymmetric str.), 1253 and 1220 (Ar. C−O str.), 1192 H−C−O−C (torsion in the oxazing ring), 1074 (furan C−O asymmetric stretching), 1057−1020 (aliphatic C−O str.), 927−910 (oxazine related band), 870 (1,2,4,5-C−H out-of-plane deformation in tetrasubstituted benzenes), 742 (furan out-of-plane in-phase wagging deformation).

HR-MS (EI) m/z, $[M]^+$ calculated for $C_{14}H_{13}NO_4^+$, 259.08446; found, 259.08511.

Polymerization. Polymerization of 7-(furan-2-ylmethyl)-7,8-dihydro-6*H*-[1,3]dioxolo[4′,5′:4,5]benzo[1,2-*e*][1,3]oxazine (**S-fa**) was carried out following a stepwise process. First, each sample was heated from room temperature to 150 °C at a heating rate of 10 °C/min. Samples were kept at this temperature for 1 min, ensuring full melting of the monomer crystals. Then, the temperature was increased to 227 °C, at the same heating rate of 10 °C/min. Lastly, samples were polymerized for 30 min at this temperature, which corresponds to the onset of the polymerization of **S-fa**, as calculated from the DSC analysis.

Characterization Methods. ^{1}H NMR spectra were acquired on a Varian Oxford AS600 at a proton resonance frequency of 600 MHz and the corresponding carbon resonance frequency of 150.8652 MHz. The average number of transients for ^{1}H measurement was 32. A relaxation time of 10 s was used for the integrated intensity determination of ^{1}H NMR spectra. 2D ^{1}H−^{13}C heteronuclear single quantum correlation (HSQC) experiments were recorded on a Bruker Ascend III 500 MHz NMR spectrometer equipped with a prodigy probe at a proton resonance frequency of 500 MHz. Parameters used were 2048 data points along the f2 dimension, 256 free induction decays in the f1 dimension, pulse width 11.05 ms, spectral width 3448 Hz (1 H), number of scans 16, digital resolution 1.68 Hz per point, relaxation delay between 1 and 10 s, and mixing times between 500 and 900 ms. Experiments were performed at 25 °C in DMSO-d_6. The data were zero-filled in the f1 dimension before Fourier transformation. Apodization using a sine-squared bell window function was applied before processing the free induction decay (FID).

FT-IR spectra were recorded using a Bomem Michelson MB100 FT-IR spectrometer equipped with a deuterated triglycine sulfate (DTGS) detector and a dry air purge unit. Co-addition of 64 scans was recorded at a resolution of 4 cm^{-1}.

A TA Instruments differential scanning calorimeter (DSC) model 2920 was used with a heating rate of 10 °C min^{-1} from room temperature to 300 °C and a nitrogen flow rate of 60 mL min^{-1} for conventional DSC studies. To calculate the polymerization activation energy of **S-fa**, samples were scanned at the different heating rates of 2, 5, 10, 15, and 20 °C/min. In all cases, all samples (1.8 ± 0.2 mg) were sealed in hermetic aluminum pans with lids.

Conventional thermogravimetric analysis (TGA) was performed using TA Instruments model Q500 TGA with a heating rate of 10 °C/min from room temperature to 800 °C and a nitrogen flow rate of 60 mL/min. To calculate the activation energy of the thermal decomposition of **poly(S-fa)**, samples (8.1 ± 0.5 mg) were scanned at the different heating rates of 2, 5, 10, 20, and 40 °C/min using a Shimadzu Instruments model TGA-50. All thermal analyses and polymerization were carried out under nitrogen atmosphere.

High-resolution mass spectrometry (HR-MS) analysis was conducted on a Kratos MS-25 mass spectrometer using electron

DOI: 10.1021/acssuschemeng.8b02641
ACS Sustainable Chem. Eng. 2018, 6, 13096−13106

impact (EI) as ionization source, at 150 °C, electron energy of 28 eV, and in positive mode.

RESULTS AND DISCUSSION

A mono-oxazine benzoxazine monomer using sesamol and furfurylamine, **S-fa**, was synthesized using ethanol and ethyl acetate, which are greener than the reported common solvents used to date in the preparation of benzoxazines (Scheme 1). The yields of **S-fa** were 72 and 68% using ethanol and ethyl acetate as the solvent, respectively.

Chemical structure of **S-fa** was characterized by combining FT-IR, ^{1}H NMR, ^{13}C NMR, and HSQC spectroscopies as well as high-resolution mass spectrometry (HR-MS). It is important to note that this synthesis might produce either of the two or both possible isomers shown in Scheme 1.

FT-IR spectrum of **S-fa** is shown in Figure 1. Due to their structural similarities, the vibrational modes of some specific

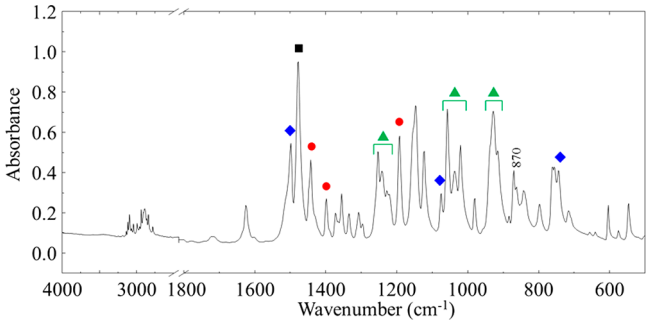

Figure 1. FT-IR spectrum of **S-fa**. (●) Characteristic absorption bands exclusively due to the benzoxazine moiety, (■) characteristic absorption bands exclusively due to the sesamol moiety, (◆) characteristic absorption bands exclusively due to the furfural moiety, and (▲) characteristic absorption bands are simultaneously due to both the benzoxazine and sesamol moieties.

groups in benzoxazine and methylenedioxybenzene compounds give rise to proximate characteristic bands, which makes its assignment difficult. In fact, stretching vibrations of different aromatic C−O linkages are assigned from bands observed between 1253 and 1220 cm^{-1}, as well as the characteristic bands observed in the region from 1057 to 1020 cm^{-1} due to the aliphatic C−O stretching vibration of aryl ethers. Similarly, the region from 960 to 890 cm^{-1} exhibits characteristic absorption bands simultaneously due to both the benzoxazine and sesamol moieties. Thus, the characteristic absorption bands associated with the C−O stretching mode of the oxazine ring and phenolic ring vibrational modes in benzoxazines,[47] and that of the most characteristic methylenedioxy[48] groups, are centered at 929 and 920 cm^{-1}. Fortunately, some characteristic bands belonging to both benzoxazine and methylenedioxybenzene moieties could be identified. Thus, bands at 1442, 1398, and 1192 cm^{-1} were assigned to CH_2 bending, C−N−C antisymmetric stretching, and H−C−O−C torsion in the oxazing ring, respectively. The very strong band observed at 1477 cm^{-1}, found in most of the methylenedioxy compounds,[49] is assigned to the CH_2 bending of the methylenedioxybenzene group. Additionally, confirmation of the oxazine ring-closure reaction is clearly observed in the characteristic band at 870 cm^{-1} due to 1,2,4,5-C−H out-of-plane deformation in tetrasubstituted benzenes. Moreover, furan moiety is indicated by the characteristic bands found at 1498, 1074, and 742 cm^{-1}, which are originated from C═C stretching, C−O−C antisymmetric stretching, and out-of-plane in-phase wagging deformation, respectively.

Figure 2 shows the ^{1}H NMR spectrum of **S-fa**. The nomenclature used for this analysis is indicated in Figures 2 and 3.

The ^{1}H NMR spectrum in Figure 2 shows the characteristic signals for benzoxazines, corresponding to the two methylenes in the oxazine ring. The peak at 4.74 ppm is assigned to O−CH_2−N, also known as the proton at the 2-position. The resonance signals for Ar−CH_2−N and N−CH_2−furan, protons at the 4- and a-positions, around 3.8 ppm, are heavily overlapped. This overlapping is easily confirmed by the integration value, which corresponds to four protons. However, both of these signals are supposed to be singlets, and the resolution of the spectrum is high enough to let us see the maximum of each of those signals, as shown in the inset. Thus, it would be fairly simple to unambiguously assign each of

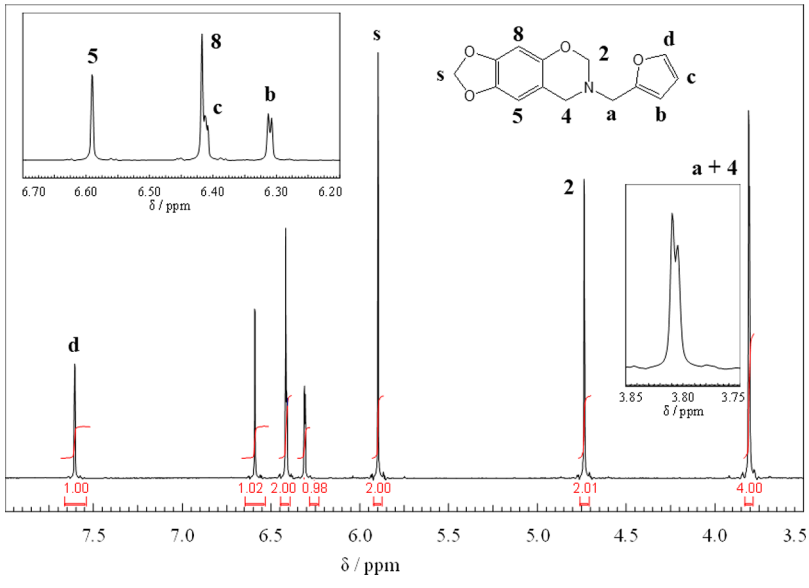

Figure 2. ^{1}H NMR of **S-fa** in DMSO-d_6.

DOI: 10.1021/acssuschemeng.8b02641
ACS Sustainable Chem. Eng. 2018, 6, 13096−13106

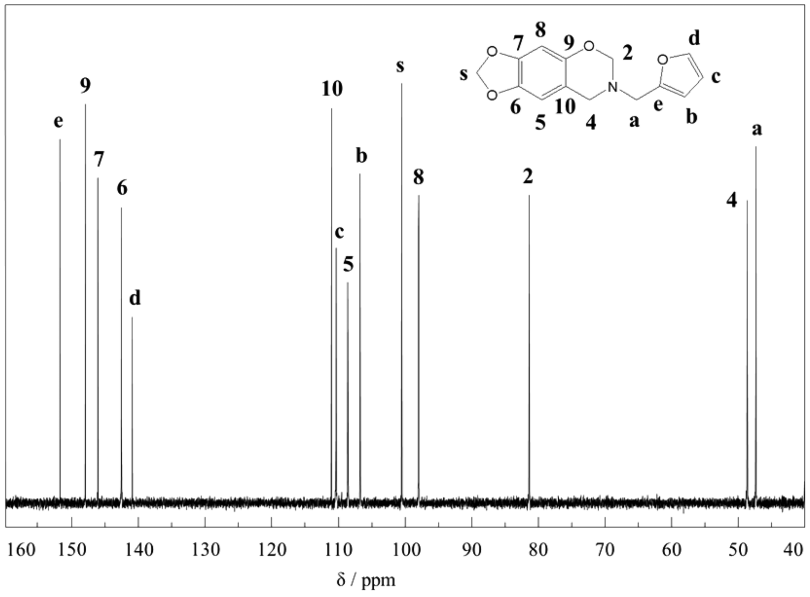

Figure 3. ^{13}C NMR spectrum of **S-fa** in DMSO-d_6.

those signals if after fully interpreting the corresponding ^{13}C NMR (presented next and in Figure 3) a fully detailed analysis by HSQC is realized (Figure 4).

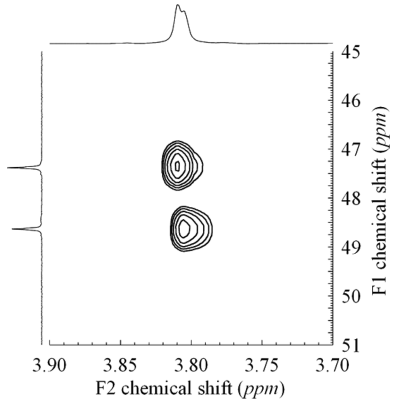

Figure 4. Region between 3.90 and 3.70 ppm in the ^{1}H axis and between 51 and 45 ppm in the ^{13}C axis in the HSQC spectrum of **S-fa** in DMSO-d_6.

The C_s, which is a methylene group between two oxygen atoms (O−CH_2−O), is observed at 5.90 ppm. Furan resonances present spin coupling, and the three signals are seen as a doublet at 7.61 ppm, a doublet of doublet at 6.41 ppm, and a doublet at 6.31 ppm for H_d, H_c, and H_b, respectively. The aromatic signals were crucial to determining the conformation of the isomer obtained in the synthesis. The only possible conformation for a tetra-substituted aromatic ring that produces two singlet signals with a 1:1 integration ratio, as seen in Figure 2, is one where the two protons are located in the *para* position with respect to each other. The singlet signal at 6.42 ppm corresponds to H_8, which appears at lower field when compared to H_5 (6.59 ppm) because of the shielding effect caused by two oxygen atoms in *β*-position with respect to the given positions. Additionally, the complete absence of two extra doublet signals in the aromatic region corresponding to two single protons in an aromatic ring in the *ortho* position with regard to each other show that no other isomer of this compound was obtained following the synthetic procedure herein described. These results not only confirm that only one isomer is obtained but also show the right configuration of the isomeric form in which **S-fa** is obtained following the synthetic procedure described in this work.

Figure 3 shows the ^{13}C NMR spectrum of **S-fa**, in which the numbering for the remaining position where no protons are present is completed.

The presence of the oxazine ring fused to the benzene ring was verified by the characteristic resonance signals in ^{13}C NMR observed at 81.38 and 48.68 ppm, which are assigned to C_2 (O−CH_2−N) and C_4 (Ar−CH_2−N), respectively. The signal corresponding to C_a (N−CH_2−furan) is seen at lower field (47.38 ppm) than that of C_4, which is a member of the 6-membered oxazine ring. The resonance of C_s (O−CH_2−O) is observed at a much higher field value (100.50 ppm) than those of the previous cases. This shifting to higher fields is not only because this carbon is part of a more restricted, stressed, and hindered 5-membered heterocycle but also because it is directly bonded to two very electronegative oxygen atoms, producing a strong deshielding effect.

The sp^2 carbons can be divided into two groups: the ones directly bonded to an oxygen atom (C_6, C_7, C_9, C_e, and C_d) and the ones that are not (C_5, C_8, C_{10}, C_b, and C_c). The presence of an oxygen atom directly bonded to the carbon induces shifting of the signals toward higher fields (observed between 141 and 152 ppm in our case) because of the deshielding produced on the carbon atoms through an inductive effect. Signals in this range are assigned as follows: C_e (151.82 ppm), C_9 (148.01 ppm), C_7 (146.13 ppm), C_6 (142.61 ppm), and C_d (141.00 ppm).

For the second group of sp^2 carbons, C_8 is the one that appears at the lower field value because of the shielding effect of two oxygen atoms in the *β*-position, while C_5 has only one oxygen atom in the *β*-position. In the case of C_{10}, which bears one oxygen atom in the *β*-position, the methylene amine group directly bonded to this carbon induces a deshielding effect over this position, thus shifting its signal to higher fields. The relative order in this case is C_{10} (111.08 ppm), C_5 (108.60 ppm), and C_8 (97.98 ppm). Finally, the two remaining

DOI: 10.1021/acssuschemeng.8b02641
ACS Sustainable Chem. Eng. 2018, 6, 13096−13106

resonance signals are C_c and C_b, which are observed at 110.38 and 106.76 ppm, respectively. It is worth mentioning that these results are in agreement with those from ^{1}H NMR analysis, demonstrating that only one isomer of **S-fa** is obtained, whose structure is shown in Figure 3, following the synthetic procedure herein described. It must be pointed out that obtaining only one isomer when reacting sesamol, by substituting one hydrogen atom on its aromatic ring, is actually the most normal reaction product and is independent of the reaction itself.[50−55] Therefore, the formation of only one isomer of **S-fa** was somehow expected.

Having fully interpreted the ^{13}C NMR, it is now possible to finish the unambiguous assignment of the two overlapped signals belonging to those protons in the 4- and a-positions, by elucidating the HSQC spectrum. This is possible because the HSQC experiment helps to elucidate proton−carbon single-bond correlations. The region between 3.90 and 3.70 ppm in the ^{1}H axis and between 51 and 45 ppm in the ^{13}C axis of the HSQC spectrum of **S-fa** is presented in Figure 4.

The correlation between the resonance signal for C_4 (48.68 ppm) and the signal at 3.80 ppm indicates that this signal corresponds to the proton at the 4-position, Ar−CH_2−N. A similar correlation is observed between the resonance of signal C_a (47.38 ppm) and the one at 3.81 ppm corresponding to H at the a-position, N−CH_2−furan.

At this point, and from the aforementioned spectroscopic techniques, the chemical structure of the new benzoxazine, **S-fa**, was successfully and unambiguously elucidated.

The polymerization behavior of **S-fa** was monitored by DSC as shown in Figure 5.

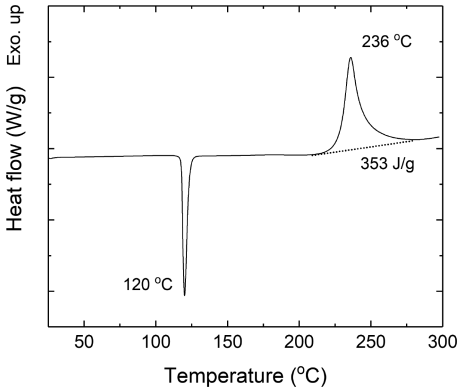

Figure 5. DSC thermogram of **S-fa** carried out from 25 to 300 °C. The endothermic peak centered at 120 °C is attributed to the melting, while the exothermic one with a maximum at 236 °C is attributed to the polymerization of **S-fa**.

The thermogram of **S-fa** shows different thermal events. The first one is detected through a very sharp and highly symmetric endothermic peak with its minimum centered at 120 °C. Then, there is an exothermic peak with a maximum at 236 °C, which is overlapped with an additional exothermic event observed at a slightly higher temperature. It is worth mentioning that there is a wide temperature gap between the endothermic and exothermic events, suggesting that this resin will have a wide processing window.

The endothermic peak is attributed to the melting of the pure needle-like single crystals of the resin (see Figure 6). The actual half-width of this sharp and symmetric melting peak was measured from the original data and corresponds to 3 °C for

Figure 6. Needle-like crystals of **S-fa** obtained after purification by recrystallization.

DSC measurements carried out at a heating rate of 10 °C on samples of 1.8 ± 0.2 mg. The combination of the aspect ratio of the melting peak with the more quantitative value of the peak half-width of this endothermic event, which in fact are fully reproducible, are strong indications of the high purity of **S-fa**.[9,56−58] Further corroborating evidence of the high purity of **S-fa** was obtained by HR-MS as no peaks other than the molecular ion and protonated molecular ion peaks were detected (Table 2). Regarding the exothermic events, the main

Table 2. HR-MS Results of S-fa

formula	calculated	found	Relative abundance (%)
$C_{14}H_{13}NO_4^+$	259.08446	259.08511	100
$[C_{14}H_{13}NO_4]H^+$	260.09228	260.09211	13

exothermic peak with maximum at 236 °C and onset at 227 °C is associated with the polymerization of **S-fa**, whereas the following overlapped extra and also exothermic event is assumed to be postpolymerization reactions. The latter ones might involve the furfuryl group, which has been reported to react in this range of temperatures under similar conditions.[25] In fact, it has recently been smartly included as a part of the chemical structures of other benzoxazine resins to induce this reactivity under similar conditions.[21]

The DSC exothermic peak temperature as a function of the heating rate for the polymerization reaction of **S-fa** was plotted according to the Kissinger[59] and Ozawa[60] equations as follows in order to determine the activation energy of polymerization (Figure 7). The Kissinger and the modified Ozawa equations[61] are shown as follows,

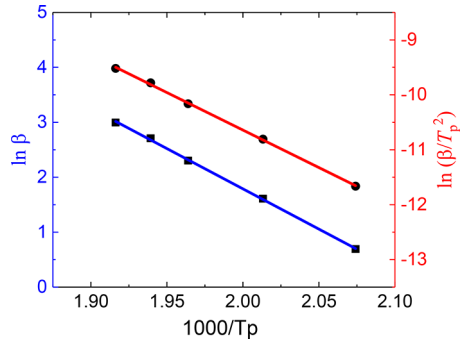

Figure 7. Plots to graphically calculate the activation energy (E_a) of the polymerization reaction of **S-fa** applying the Kissinger and modified Ozawa methods. Linear regressions obtained for each method are R^2 = 0.9994 for the Kissinger method (● and red line) and R^2 = 0.9995 for the Ozawa method (■ and blue line).

DOI: 10.1021/acssuschemeng.8b02641
ACS Sustainable Chem. Eng. 2018, 6, 13096−13106

$$\ln\left(\frac{\beta}{T_p^2}\right) = \ln\left(\frac{AR}{E_a}\right) - \frac{E_a}{RT_p} \quad \text{Kissinger equation} \tag{1}$$

$$\ln \beta = -1.052\frac{E_a}{RT_p} + C \quad \text{modified Ozawa equation} \tag{2}$$

where β is the constant heating rate and T_p is the maximum value of the exothermic polymerization peak. E_a is the activation energy for polymerization, R is the gas constant, and A is the frequency factor.

The results are presented in Figure 7, which shows perfect straight lines with slopes of −13.66 and −14.66 for the Kissinger and Ozawa plots, respectively. The activation energy, E_a, for the polymerization reaction of **S-fa** is easily calculated from those slopes, being 113.6 and 115.9 kJ/mol by the Kissinger and Ozawa methods, respectively. These values are in the general range of those published for other benzoxazine resins.[62−65]

As shown in Figure 7, the plots resulted in perfect straight lines in both cases. This result indicates that the polymerization of the highly purified **S-fa** follows a single polymerization mechanism. Due to the highly pure nature of the compound used, it is difficult to assume a polymerization initiation as would normally be explained by cationic impurities. However, an intrinsic and self-initiating polymerization mechanism has recently been reported.[14] The current result is consistent with this self-initiating polymerization mechanism. Moreover, it is worth noting that both plots in Figure 7 are perfectly straight lines, evidencing that the second exothermic event occurring as postpolymerization reactions has a negligible effect on the main exothermic peak.

With the interest of evaluating the herein prepared benzoxazine as a resin for obtaining a novel thermoset, and especially toward the thermal stability of the resulting polybenzoxazine, **S-fa** was polymerized. Polymerizations of **S-fa** were carried out following a four-step process as stated in the Experimental Section.

It is well-known that thermal degradation of polybenzoxazines proceeds, in general, following a three-step process.[66] These processes can be observed in thermograms obtained by TGA, which helps to evaluate the thermal stability of the samples under study. Therefore, the thermal stability of **poly(S-fa)** was examined with TGA, as shown in Figure 8.

The thermogram shown in Figure 8 can be divided into four main regions. In the first one, between room temperature and 280 °C there is very little weight loss (<1%). This event was previously reported to result from the degradation of chain ends and/or short branches. Although **S-fa** is a mono-oxazine benzoxazine resin that usually results in small oligomers upon polymerization at best, it also has structures resulting from the use of furfurylamine, which can also participate in the polymerization. This resin belongs to the class of benzoxazines that is mono-oxazine resin with additional reactive groups with nonbenzoxazine polymerization mechanism. This class of benzoxazine resin can lead to cross-linked structures. From the nearly negligible presence of this low thermic event, it is suggested that the polymerized structure has less chain ends and side chains than other polybenzoxazines derived from usual dioxazine benzoxazine monomers. In the second region, a major weight loss rate is observed between 280 and 344 °C. In the third region, a broader temperature weight loss with somewhat reduced weight-loss rate is clearly seen between 344 and 473 °C. Finally, a slow and more complex degradation profile is detected in the fourth region between 473 and 800 °C.

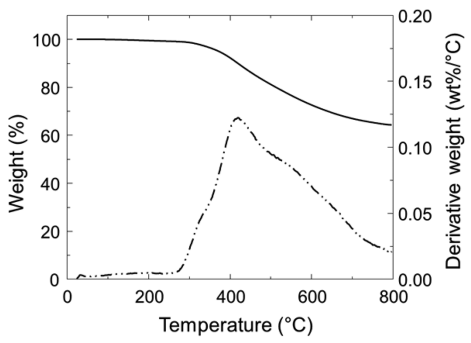

Figure 8. TGA (—) and DTG (−··) thermograms of **poly(S-fa)**.

As can be seen from the previous results, **poly(S-fa)** exhibits a high thermal stability. With the aim of corroborating that high thermal stability and making it comparable to other systems, more quantitative information is needed. Therefore, a summary of the main thermal properties, T_{d5} and T_{d10}, defined as the temperatures at which the weight loss is 5% and 10%, respectively, and char yield, defined as the residual weight at 800 °C under N_2 atmosphere, of **poly(S-fa)** obtained from TGA measurements shows the following values: T_{d5} of 374 °C, T_{d10} of 419 °C, and, of particular interest, a char yield as high as 64%. These results are evidence for the excellent thermal stability of **poly(S-fa)**. This thermal stability is rather unexpected for polybenzoxazines made from natural renewable resources. However, it is not unusual anymore because our group has already reported similar behavior for other biobased polybenzoxazines.[21,67,68]

From an applied polymer science standpoint, it was easy to realize that all thermal properties related to thermal stability exhibited by **poly(S-fa)**, which are additionally accompanied by a slow degradation profile occurring at high temperature, are indeed very desirable features of any polymer system to be considered as a good fire-resistant material.[67,69] This combination of facts further motivated us to quantitatively determine the activation energy for the thermal degradation reaction of the herein prepared **poly(S-fa)**. This result would provide further and complementary quantitative information about the possibility of using this **poly(S-fa)** or any related thermoset material or additive as a promising candidate toward applications at high temperatures. To achieve this goal, we took into consideration Kissinger's concept,[70] where he and Blaine demonstrated that the peak displacement method (nowadays also known as nonisothermal method) is indeed applicable to other thermal analytical techniques, such as TGA, by selecting appropriate points of constant conversion on the thermal curves. Thus, the graphical determination of the activation energy for the thermal degradation of **poly(S-fa)** is presented in Figure 9. The Kissinger and the modified Ozawa equations are then adapted as follows,

$$\ln\left(\frac{\beta}{T_d^2}\right) = \ln\left(\frac{AR}{E_a}\right) - \frac{E_a}{RT_d} \quad \text{Kissinger equation} \tag{3}$$

DOI: 10.1021/acssuschemeng.8b02641
ACS Sustainable Chem. Eng. 2018, 6, 13096−13106

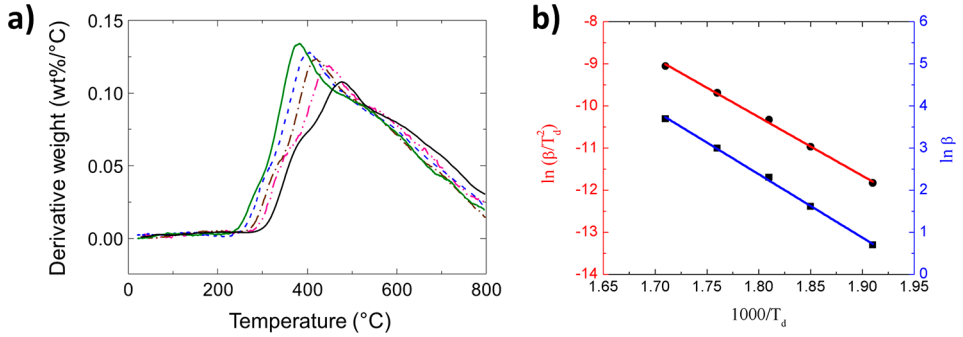

Figure 9. Plots to graphically calculate the activation energy (E_a) for the thermal degradation of **poly(S-fa)** applying the Kissinger and modified Ozawa methods. (a) Graphic of the derivative weight (wt %/°C) as a function of the temperature carried out at different heating rates, specifically 2 (green solid line), 5 (blue dashed line), 10 (brown dash-dotted line), 20 (pink dash-dotted line), and 40 °C (black solid line) on **poly(S-fa)** samples. (b) In the plots, β is the constant heating rate and T_d is the onset value of the exothermic degradation process. Linear regressions obtained for each method are R^2 = 0.9990 for the Kissinger method (● and red line) and R^2 = 0.9991 for the Ozawa method (■ and blue line).

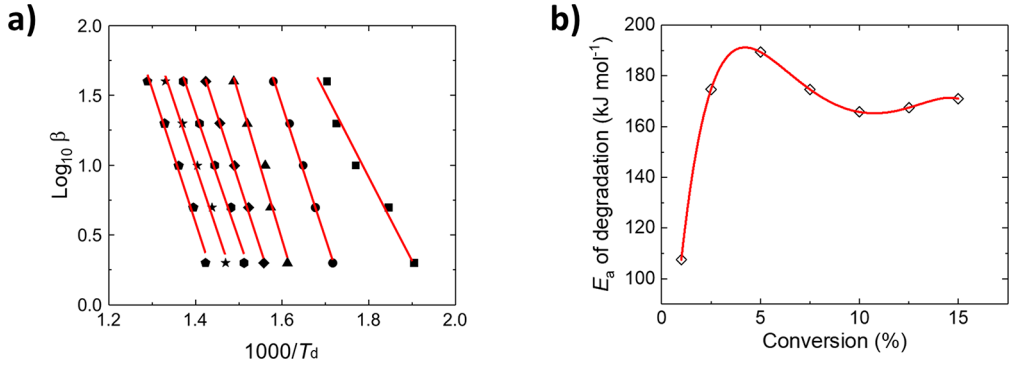

Figure 10. (a) Isoconversional plot to graphically calculate the apparent activation energy (E_a) for the thermal degradation of **poly(S-fa)** applying the Flynn–Wall–Ozawa method. Conversions: 1.0 (■), 2.5 (●), 5.0 (▲), 7.5 (◆), 10.0 (⬢), 12.5 (★), and 15.0 (solid pentagon). (b) E_a of degradation as a function of the degradation conversion of **poly(S-fa)**, at the same conversion used for the E_a of degradation calculated utilizing the Flynn–Wall–Ozawa method.

$$\ln \beta = -1.052\frac{E_a}{RT_d} + C \qquad \text{modified Ozawa equation} \tag{4}$$

where β is the constant heating rate and T_d is the degradation temperature value at a given conversion. E_a is in this case the activation energy for the thermal degradation, R is the gas constant, and A is the frequency factor.

The degradation kinetics of **poly(S-fa)** was studied using the nonisothermal TGA method at the different heating rates of 2, 5, 10, 20, and 40 °C/min. For a clearer visualization of the thermal events, only the derivative weight (wt %/°C) as a function of the temperature carried out at each mentioned heating rate is plotted and shown in Figure 9a. Using data extracted from this figure made it possible to obtain Figure 9b by plotting $\ln(\beta/T_d^2)$ as well as $\ln \beta$ as a function of $1/T_d$ according to both the Kissinger and Ozawa methods, respectively. As can be seen from the figure, a straight line was obtained in both cases, implying that the degradation process near this temperature regime is a simple and single mechanism.

The actual values of the activation energy for the degradation of **poly(S-fa)** are then obtained following the same approach as in the case of the nonisothermal method carried out using the DSC to graphically determine the activation energy for the polymerization reaction of **S-fa**.[63,70,71] In other words, the activation energy for the degradation of **poly(S-fa)** is determined from the slope of the straight lines obtained in the plots presented in Figure 9b. The slope values determined from the plots are −13.94 and −15.05 for the Kissinger and Ozawa methods, respectively. Therefore, the corresponding activation energies for the thermal degradation of **poly(S-fa)** are easily calculated as 115.9 and 118.9 kJ/mol for the Kissinger and Ozawa methods, respectively.

To complement this last result, we were also interested in carrying out the calculation of the apparent activation energy of degradation of **poly(S-fa)** but this time following the common isoconversional method known as the Flynn–Wall–Ozawa method.[60,72] This is an integral method leading to $-0.4567E_a/R$ from the slope of the straight line obtained by plotting $\log_{10} \beta$ as a function of $1000/T_d$ for a constant set of degradation conversion values obtained from TGA at different heating rates. The equation describing the Flynn–Wall–Ozawa method is

$$\log_{10} \beta = \log_{10}\left(\frac{AE_a}{R(\alpha)}\right) - 2.315 - 0.4567\frac{E_a}{RT} \qquad \text{Flynn–Wall–Ozawa equation} \tag{5}$$

where β is the constant heating rate and T is the degradation temperature value at a given conversion α. E_a is in this case the activation energy for the thermal degradation, R is the gas constant, and A is the frequency factor.

This study was carried out applying the following heating rates 2, 5, 10, 20, and 40 °C/min. The conversions at which

DOI: 10.1021/acssuschemeng.8b02641
ACS Sustainable Chem. Eng. 2018, 6, 13096−13106

each temperature were measured are 1.0, 2.5, 5.0, 7.5, 10.0, 12.5, and 15.0%. The combination of these data made possible to obtain Figure 10 by plotting $\log_{10}\beta$ as a function of $1000/T$ according to the Flynn−Wall−Ozawa method. As can be seen from Figure 10a, a straight line was obtained at each conversion studied. Similarly as for the Kissinger method, a single mechanism can be assumed if straight lines are obtained in the plots, whereas a multistep mechanism might be inferred if the relation observed between E_a of degradation and conversion is not linear.[63] Therefore, these results show again a single and simple degradation mechanism, which is in agreement with the previous results obtained following the Kissinger method.

It is generally accepted that the E_a is the necessary energy that must be provided to a system to produce the reaction under consideration. In the present case is the degradation reaction, which can take place by braking or rearranging chemical bonds throughout the chemical structure of the polymer. Figure 10b shows the apparent activation energy of degradation of **poly(S-fa)** as a function of the conversion. As can be seen from the figure, the E_a increases up to a maximum value of 191.2 kJ mol^{-1} at a conversion of ∼4.2%. From this conversion on the degradation reaction, it is somehow facilitated as the necessary energy to maintain the degradation reaction of the polymer is lower as the conversion increases. Thus, the maximum value of E_a obtained is 191.2 kJ mol^{-1}, which then might represent the main energetic barrier for the thermal degradation of **poly(S-fa)**.

The E_a values obtained by the Flynn−Wall−Ozawa method are greater than that obtained by the Kissinger method, which is in agreement with previous reported data.[73] However, what must be highlighted herein is that the apparent activation energy of degradation of **poly(S-fa)** calculated by the Flynn−Wall−Ozawa method is greater than the E_a calculated by the same method and reported for most natural fibers, such as bagasse, bamboo, cotton stalk, hemp, jute, kenaf, rice husk, wood-maple, and wood-pine exhibiting 169.5, 162.8, 169.9, 177.9, 184.2, 170.3, 167.4, 155.8, and 161.8 kJ mol^{-1}, and only exceeded by rice straw, which was shown to have an E_a of 195.9 kJ mol^{-1}.[73] The high thermal stability of **poly(S-fa)** accompanied by the slow degradation profile and the high char yield formation make this novel biobased thermoset a good candidate toward fire-resistant materials.

CONCLUSION

A fully biobased, novel sesamol−furfurylamine-containing benzoxazine, namely, **S-fa**, was designed and successfully synthesized by reacting sesamol, furfurylamine, and formaldehyde. The extra benefit developed in this synthesis methodology is the use of greener solvents than most of the synthetic pathways reported to date. Importantly, the greener solvents were successfully applied not only for carrying out the actual chemical reaction but also to perform the entire purification process. The two solvents positively evaluated for these more eco-friendly synthetic methods are ethanol and ethyl acetate, because these two solvents are classified as the most recommended solvents to be used whenever possible by the rules of Green Chemistry. It is worth noticing that the yield of the respective syntheses was not sacrificed and remained at ∼70% in both cases.

Reactivity toward polymerization was also studied. A fairly low polymerization temperature is observed for this resin. This effect is known for those benzoxazines where furfurylamine has been introduced into their chemical structures. The activation energy for the polymerization reaction of **S-fa** was carried out following the Kissinger and Ozawa methods, obtaining values in the normal range as for other benzoxazine resins.

The resulting biobased thermoset was further studied with regard to its thermal stability. **Poly(S-fa)** exhibited excellent thermal properties. On the basis of these positive results, a great interest in evaluating this novel thermoset toward future possible applications emerged immediately. Thus, the activation energy for the degradation reaction of **poly(S-fa)** was carried out following the Kissinger and Ozawa methods. The combination of the excellent thermal properties accompanied of a slow degradation profile at high temperature with an acceptable value of the activation energy of thermal degradation position the herein synthesized **poly(S-fa)** as a promising material for anti-flammable and fire resistant applications.

In summary, we have demonstrated that high-end materials can be designed and synthesized under environmentally and eco-friendly conditions using raw materials coming from natural renewable resources and only utilizing the most recommended solvents as considered by the Principles of Green Chemistry.

AUTHOR INFORMATION

Corresponding Authors

*E-mail: hxi3@case.edu.

*E-mail: pxf106@case.edu.

ORCID

Hatsuo Ishida: 0000-0002-2590-2700

Present Address

§M.L.S.: CIHIDECAR-CONICET y Departamento de Química Orgánica, Facultad de Ciencias Exactas y Naturales, Universidad de Buenos Aires, Intendente Güiraldes s/n, Pabellón II, 3er piso, Ciudad Universitaria, Buenos Aires 1428, Argentina

Notes

The authors declare no competing financial interest.

REFERENCES

(1) Ishida, H.; Froimowicz, P. *Advanced and Emerging Polybenzoxazine Science and Technology*; Elsevier Science Bv: Amsterdam, 2017; pp 1−1097.

(2) Kaewvilai, A.; Wattanathana, W.; Jongrungruangchok, S.; Veranitisagul, C.; Koonsaeng, N.; Laobuthee, A. 3,4-Dihydro-1,3−2H-benzoxazines: Novel reducing agents through one electron donation mechanism and their application as the formation of nano-metallic silver coating. *Mater. Chem. Phys.* **2015**, *167*, 9−13.

(3) Vaithilingam, S.; Jayanthi, K. P.; Muthukaruppan, A. Synthesis and characterization of cardanol based fluorescent composite for optoelectronic and antimicrobial applications. *Polymer* **2017**, *108*, 449−461.

(4) Alper-Hayta, S.; Aki-Sener, E.; Tekiner-Gulbas, B.; Yildiz, I.; Temiz-Arpaci, O.; Yalcin, I.; Altanlar, N. Synthesis, antimicrobial activity and QSARs of new benzoxazine-3-ones. *Eur. J. Med. Chem.* **2006**, *41* (12), 1398−1404.

(5) Gupta, N.; Sharma, S.; Raina, A.; Dangroo, N. A.; Bhushan, S.; Sangwan, P. L. Synthesis and anti-proliferative evaluation of novel 3,4-dihydro-2H-1,3-oxazine derivatives of bakuchiol. *RSC Adv.* **2016**, *6* (108), 106150−106159.

(6) Ning, X.; Ishida, H. Phenolic materials via ring-opening polymerization - synthesis and characterization of bisphenol-a based benzoxazines and their polymers. *J. Polym. Sci., Part A: Polym. Chem.* **1994**, *32* (6), 1121−1129.

DOI: 10.1021/acssuschemeng.8b02641
ACS Sustainable Chem. Eng. 2018, 6, 13096−13106

(7) Verge, P.; Puchot, L.; Vancaeyzeele, C.; Vidal, F.; Habibi, Y. Symmetric Versus Asymmetric di-Bz Monomer Design: Structure-to-Properties Relationship. In *Advanced and Emerging Polybenzoxazine Science and Technology*; Ishida, H., Froimowicz, P., Eds.; Elsevier Science Bv: Amsterdam, 2017; pp 89−107; DOI: 10.1016/b978-0-12-804170-3.00007-x.
(8) Zhang, K.; Froimowicz, P.; Ishida, H. Development of New Generation Benzoxazine Thermosets Based on Smart Ortho-Benzoxazine Chemistry. In *Advanced and Emerging Polybenzoxazine Science and Technology*; Ishida, H., Froimowicz, P., Eds.; Elsevier Science Bv: Amsterdam, 2017; pp 35−64; DOI: 10.1016/b978-0-12-804170-3.00004-4.
(9) Zhang, W. F.; Froimowicz, P.; Arza, C. R.; Ohashi, S.; Xin, Z.; Ishida, H. Latent Catalyst-Containing Naphthoxazine: Synthesis and Effects on Ring-Opening Polymerization. *Macromolecules* **2016**, *49* (19), 7129−7140.
(10) Froimowicz, P.; Zhang, K.; Ishida, H. Intramolecular Hydrogen Bonding in Benzoxazines: When Structural Design Becomes Functional. *Chem. - Eur. J.* **2016**, *22* (8), 2691−2707.
(11) Lorjai, P.; Wongkasemjit, S.; Chaisuwan, T.; Jamieson, A. M. Significant enhancement of thermal stability in the non-oxidative thermal degradation of bisphenol-A/aniline based polybenzoxazine aerogel. *Polym. Degrad. Stab.* **2011**, *96* (4), 708−718.
(12) Zhu, Y. F.; Gu, Y. Effect of Interaction between Transition Metal Oxides and Nitrogen Atoms on Thermal Stability of Polybenzoxazine. *J. Macromol. Sci., Part B: Phys.* **2011**, *50* (6), 1130−1143.
(13) Ran, Q. C.; Zhang, D. X.; Zhu, R. Q.; Gu, Y. The structural transformation during polymerization of benzoxazine/FeCl3 and the effect on the thermal stability. *Polymer* **2012**, *53* (19), 4119−4127.
(14) Han, L.; Salum, M. L.; Zhang, K.; Froimowicz, P.; Ishida, H. Intrinsic self-initiating thermal ring-opening polymerization of 1,3-benzoxazines without the influence of impurities using very high purity crystals. *J. Polym. Sci., Part A: Polym. Chem.* **2017**, *55* (20), 3434−3445.
(15) Kiskan, B. Adapting benzoxazine chemistry for unconventional applications. *React. Funct. Polym.* **2018**, *129*, 76−88.
(16) Chiou, K.; Froimowicz, P.; Landfester, K.; Taden, A.; Ishida, H. Triggered Precision Benzoxazine Film Formation by Thermally Induced Destabilization of Benzoxazine Nanodroplets Using a LCST-Bearing Surfactant. *Macromolecules* **2014**, *47* (10), 3297−3305.
(17) Agag, T.; Liu, J.; Graf, R.; Spiess, H. W.; Ishida, H. Benzoxazole Resin: A Novel Class of Thermoset Polymer via Smart Benzoxazine Resin. *Macromolecules* **2012**, *45* (22), 8991−8997.
(18) Taskin, O. S.; Kiskan, B.; Yagci, Y. Polybenzoxazine Precursors As Self-Healing Agents for Polysulfones. *Macromolecules* **2013**, *46* (22), 8773−8778.
(19) Likitaporn, C.; Rimdusit, S. Characterizations of silicon carbide whisker-filled in benzoxazine-epoxy shape memory polymers. *Key Eng. Mater.* **2015**, *659*, 373−377.
(20) Chiou, K.; Ishida, H. Incorporation of Natural Renewable Components and Waste Byproducts to Benzoxazine Based High Performance Materials. *Curr. Org. Chem.* **2013**, *17* (9), 913−925.
(21) Froimowicz, P.; Arza, C. R.; Han, L.; Ishida, H. Smart, Sustainable, and Ecofriendly Chemical Design of Fully Bio-Based Thermally Stable Thermosets Based on Benzoxazine Chemistry. *ChemSusChem* **2016**, *9* (15), 1921−1928.
(22) Anastas, P. T.; Warner, J. C. *Green Chemistry: Theory and Practice*; Oxford University Press: 2000; p 152.
(23) Capello, C.; Fischer, U.; Hungerbuhler, K. What is a green solvent? A comprehensive framework for the environmental assessment of solvents. *Green Chem.* **2007**, *9* (9), 927−934.
(24) Prat, D.; Hayler, J.; Wells, A. A survey of solvent selection guides. *Green Chem.* **2014**, *16* (10), 4546−4551.
(25) Wang, C. F.; Sun, J. Q.; Liu, X. D.; Sudo, A.; Endo, T. Synthesis and copolymerization of fully bio-based benzoxazines from guaiacol, furfurylamine and stearylamine. *Green Chem.* **2012**, *14* (10), 2799−2806.
(26) Wang, C. F.; Zhao, C. H.; Sun, J. Q.; Huang, S. Q.; Liu, X. D.; Endo, T. Synthesis and thermal properties of a bio-based polybenzoxazine with curing promoter. *J. Polym. Sci., Part A: Polym. Chem.* **2013**, *51* (9), 2016−2023.
(27) Dumas, L.; Bonnaud, L.; Olivier, M.; Poorteman, M.; Dubois, P. Arbutin-based benzoxazine: en route to an intrinsic water soluble biobased resin. *Green Chem.* **2016**, *18* (18), 4954−4960.
(28) Kimura, H.; Murata, Y.; Matsumoto, A.; Hasegawa, K.; Ohtsuka, K.; Fukuda, A. New thermosetting resin from terpenediphenol-based benzoxazine and epoxy resin. *J. Appl. Polym. Sci.* **1999**, *74* (9), 2266−2273.
(29) Kiskan, B.; Yagci, Y. Thermally curable benzoxazine monomer with a photodimerizable coumarin group. *J. Polym. Sci., Part A: Polym. Chem.* **2007**, *45* (9), 1670−1676.
(30) Calo, E.; Maffezzoli, A.; Mele, G.; Martina, F.; Mazzetto, S. E.; Tarzia, A.; Stifani, C. Synthesis of a novel cardanol-based benzoxazine monomer and environmentally sustainable production of polymers and bio-composites. *Green Chem.* **2007**, *9* (7), 754−759.
(31) Minigher, A.; Benedetti, E.; De Giacomo, O.; Campaner, P.; Aroulmoji, V. Synthesis and Characterization of Novel Cardanol Based Benzoxazines. *Nat. Prod. Commun.* **2009**, *4* (4), 521−528.
(32) Lochab, B.; Varma, I. K.; Bijwe, J. Thermal behaviour of cardanol-based benzoxazines. *J. Therm. Anal. Calorim.* **2010**, *102* (2), 769−774.
(33) Rao, B. S.; Palanisamy, A. Monofunctional benzoxazine from cardanol for bio-composite applications. *React. Funct. Polym.* **2011**, *71* (2), 148−154.
(34) Zuniga, C.; Larrechi, M. S.; Lligadas, G.; Ronda, J. C.; Galia, M.; Cadiz, V. Polybenzoxazines from Renewable Diphenolic Acid. *J. Polym. Sci., Part A: Polym. Chem.* **2011**, *49* (5), 1219−1227.
(35) Sudo, A.; Kudoh, R.; Endo, T. Functional Benzoxazines Containing Ammonium Salt of Carboxylic Acid: Synthesis and Highly Activated Thermally Induced Ring-Opening Polymerization. *J. Polym. Sci., Part A: Polym. Chem.* **2011**, *49* (7), 1724−1729.
(36) Agag, T.; An, S. Y.; Ishida, H. 1,3-Bis(benzoxazine) from Cashew Nut Shell Oil and Diaminodiphenyl Methane and Its Composites with Wood Flour. *J. Appl. Polym. Sci.* **2013**, *127* (4), 2710−2714.
(37) Xu, H. L.; Lu, Z. J.; Zhang, G. Z. Synthesis and properties of thermosetting resin based on urushiol. *RSC Adv.* **2012**, *2* (7), 2768−2772.
(38) Comi, M.; Lligadas, G.; Ronda, J. C.; Galia, M.; Cadiz, V. Renewable Benzoxazine Monomers from "Lignin-like" Naturally Occurring Phenolic Derivatives. *J. Polym. Sci., Part A: Polym. Chem.* **2013**, *51* (22), 4894−4903.
(39) Thirukumaran, P.; Shakila, A.; Muthusamy, S. Synthesis and characterization of novel bio-based benzoxazines from eugenol. *RSC Adv.* **2014**, *4* (16), 7959−7966.
(40) Thirukumaran, P.; Shakila Parveen, A.; Sarojadevi, M. Synthesis and Copolymerization of Fully Biobased Benzoxazines from Renewable Resources. *ACS Sustainable Chem. Eng.* **2014**, *2* (12), 2790−2801.
(41) Li, S. F.; Zou, T.; Liu, X. L.; Tao, M. Synthesis and characterization of benzoxazine monomers from rosin and their thermal polymerization. *Des. Monomers Polym.* **2014**, *17* (1), 40−46.
(42) Dumas, L.; Bonnaud, L.; Olivier, M.; Poorteman, M.; Dubois, P. Bio-based high performance thermosets: Stabilization and reinforcement of eugenol-based benzoxazine networks with BMI and CNT. *Eur. Polym. J.* **2015**, *67*, 494−502.
(43) Thirukumaran, P.; Sathiyamoorthi, R.; Shakila Parveen, A.; Sarojadevi, M. New benzoxazines from renewable resources for green composite applications. *Polym. Compos.* **2016**, *37* (2), 573−582.
(44) Dumas, L.; Bonnaud, L.; Olivier, M.; Poorteman, M.; Dubois, P. Chavicol benzoxazine: Ultrahigh Tg biobased thermoset with tunable extended network. *Eur. Polym. J.* **2016**, *81*, 337−346.
(45) Fukuda, Y.; Osawa, T.; Namiki, M.; Ozaki, T. Studies on antioxidative substances in sesame seed. *Agric. Biol. Chem.* **1985**, *49* (2), 301−306.

DOI: 10.1021/acssuschemeng.8b02641
ACS Sustainable Chem. Eng. 2018, 6, 13096−13106

(46) Mariscal, R.; Maireles-Torres, P.; Ojeda, M.; Sadaba, I.; Lopez Granados, M. Furfural: a renewable and versatile platform molecule for the synthesis of chemicals and fuels. *Energy Environ. Sci.* **2016**, *9* (4), 1144−1189.
(47) Han, L.; Iguchi, D.; Gil, P.; Heyl, T. R.; Sedwick, V. M.; Arza, C. R.; Ohashi, S.; Lacks, D. J.; Ishida, H. Oxazine Ring-Related Vibrational Modes of Benzoxazine Monomers Using Fully Aromatically Substituted, Deuterated, N-15 Isotope Exchanged, and Oxazine-Ring-Substituted Compounds and Theoretical Calculations. *J. Phys. Chem. A* **2017**, *121* (33), 6269−6282.
(48) Mirghani, M. E. S.; Man, Y. B. C.; Jinap, S.; Baharin, B. S.; Bakar, J. Application of FTIR spectroscopy in determining sesamol in sesame seed oil. *J. Am. Oil Chem. Soc.* **2003**, *80* (1), 1−4.
(49) Briggs, L. H.; Colebrook, L. D.; Fales, H. M.; Wildman, W. C. Infrared absorption spectra of methylenedioxy and aryl ether groups. *Anal. Chem.* **1957**, *29* (6), 904−911.
(50) Ye, Y. Q.; Koshino, H.; Onose, J. I.; Yoshikawa, K.; Abe, N.; Takahashi, S. First total synthesis of vialinin A, a novel and extremely potent inhibitor of TNF-α production. *Org. Lett.* **2007**, *9* (21), 4131−4134.
(51) Ye, Y. Q.; Koshino, H.; Onose, J. I.; Yoshikawa, K.; Abe, N.; Takahashi, S. Expeditious synthesis of vialinin B, an extremely potent inhibitor of TNF-aα production. *Org. Lett.* **2009**, *11* (21), 5074−5077.
(52) Zhang, H.; Liao, Y. H.; Yuan, W. C.; Zhang, X. M. Organocatalytic Enantioselective Friedel-Crafts alkylation of sesamol with nitro olefins. *Eur. J. Org. Chem.* **2010**, *2010*, 3215−3218.
(53) Kumari, P.; Nandi, S.; Kumar, G.; Khan, N. H.; Kureshy, R. I.; Abdi, S. H. R.; Suresh, E.; Bajaj, H. C. Construction of highly enantioselective spiro-oxindole derivatives with fused chromene: Via organocascade catalysis. *RSC Adv.* **2016**, *6* (57), 52384−52390.
(54) Tseng, T. H.; Tsheng, Y. M.; Lee, Y. J.; Hsu, H. L. Total synthesis of carpacin and its geometric isomer as a cancer chemopreventer. *J. Chin. Chem. Soc.* **2000**, *47* (5), 1165−1169.
(55) Kumazawa, S.; Koike, M.; Usui, Y.; Nakayama, T.; Fukuda, Y. Isolation of Sesaminols as Antioxidative Components from Roasted Sesame Seed Oil. *J. Oleo Sci.* **2003**, *52* (6), 303−307.
(56) Ohashi, S.; Zhang, K.; Ran, Q.; Arza, C. R.; Froimowicz, P.; Ishida, H. Preparation of High Purity Samples, Effect of Purity on Properties, and FT-IR, Raman, ^{1}H and ^{13}C NMR, and DSC Data of Highly Purified Benzoxazine Monomers. In *Advanced and Emerging Polybenzoxazine Science and Technology*; Ishida, H., Froimowicz, P., Eds.; Elsevier Science Bv: Amsterdam, 2017; pp 1053−1082; DOI: 10.1016/b978-0-12-804170-3.00049-4.
(57) Giron, D.; Goldbronn, C. Place of dsc purity analysis in pharmaceutical development. *J. Therm. Anal.* **1995**, *44* (1), 217−251.
(58) Biltonen, R. L.; Lichtenberg, D. The use of differential scanning calorimetry as a tool to characterize liposome preparationS. *Chem. Phys. Lipids* **1993**, *64* (1−3), 129−142.
(59) Kissinger, H. E. Reaction kinetics in differential thermal analysis. *Anal. Chem.* **1957**, *29* (11), 1702−1706.
(60) Ozawa, T. A new method of analyzing thermogravimetric data. *Bull. Chem. Soc. Jpn.* **1965**, *38* (11), 1881−1886.
(61) Matusita, K.; Komatsu, T.; Yokota, R. Kinetics of non-isothermal crystallization process and activation-energy for crystal-growth in amorphous materials. *J. Mater. Sci.* **1984**, *19* (1), 291−296.
(62) Ishida, H.; Rodriguez, Y. Curing kinetics of a new benzoxazine-based phenolic resin by differential scanning calorimetrY. *Polymer* **1995**, *36* (16), 3151−3158.
(63) Liu, X. X.; Yu, L.; Xie, F. W.; Li, M.; Chen, L.; Li, X. X. Kinetics and mechanism of thermal decomposition of cornstarches with different amylose/amylopectin ratios. *Starch-Starke* **2010**, *62* (3−4), 139−146.
(64) Lu, Y. B.; Li, M. M.; Zhang, Y. J.; Hu, D.; Ke, L. L.; Xu, W. J. Synthesis and curing kinetics of benzoxazine containing fluorene and furan groups. *Thermochim. Acta* **2011**, *515* (1−2), 32−37.
(65) Zhang, K.; Zhuang, Q. X.; Zhou, Y. C.; Liu, X. Y.; Yang, G.; Han, Z. W. Preparation and properties of novel low dielectric constant benzoxazole-based polybenzoxazine. *J. Polym. Sci., Part A: Polym. Chem.* **2012**, *50* (24), 5115−5123.
(66) Liu, J.; Ishida, H. Anomalous Isomeric Effect on the Properties of Bisphenol F-based Benzoxazines: Toward the Molecular Design for Higher Performance. *Macromolecules* **2014**, *47* (16), 5682−5690.
(67) Rodriguez Arza, C.; Froimowicz, P.; Ishida, H. Smart chemical design incorporating umbelliferone as natural renewable resource toward the preparation of thermally stable thermosets materials based on benzoxazine chemistry. *RSC Adv.* **2015**, *5* (118), 97855−97861.
(68) Froimowicz, P.; Rodriguez Arza, C.; Ohashi, S.; Ishida, H. Tailor-Made and Chemically Designed Synthesis of Coumarin-Containing Benzoxazines and Their Reactivity Study Toward Their Thermosets. *J. Polym. Sci., Part A: Polym. Chem.* **2016**, *54* (10), 1428−1435.
(69) Van, A.; Chiou, K.; Ishida, H. Use of renewable resource vanillin for the preparation of benzoxazine resin and reactive monomeric surfactant containing oxazine ring. *Polymer* **2014**, *55* (6), 1443−1451.
(70) Blaine, R. L.; Kissinger, H. E. Homer Kissinger and the Kissinger equation. *Thermochim. Acta* **2012**, *540*, 1−6.
(71) Batista, N. L.; Costa, M. L.; Iha, K.; Botelho, E. C. Thermal degradation and lifetime estimation of poly(ether imide)/carbon fiber composites. *J. Thermoplast. Compos. Mater.* **2015**, *28* (2), 265−274.
(72) Flynn, J. H.; Wall, L. A. General treatment of thermogravimetry of polymers. *J. Res. Natl. Bur. Stand., Sect. A* **1966**, *70A* (6), 487−523.
(73) Yao, F.; Wu, Q. L.; Lei, Y.; Guo, W. H.; Xu, Y. J. Thermal decomposition kinetics of natural fibers: Activation energy with dynamic thermogravimetric analysis. *Polym. Degrad. Stab.* **2008**, *93* (1), 90−98.

DOI: 10.1021/acssuschemeng.8b02641
ACS Sustainable Chem. Eng. 2018, 6, 13096−13106